

# PORE WATER CHEMISTRY, MICROBIAL PROCESSES, AND TRACE METAL MOBILITY OF BIOLUMINESCENT BAYS

HILARY I. PALEVSKY

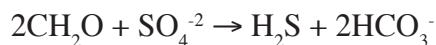
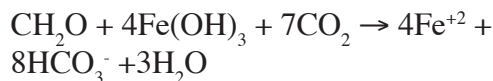
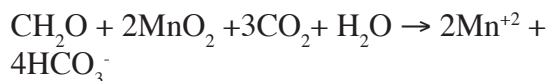
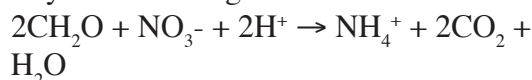
Amherst College

Anna M. Martini

## BACKGROUND

The population of dinoflagellates in the bioluminescent bays of Vieques may be controlled by environmental factors including nutrient and metal cycling, both of which are in turn dominantly controlled by microbial processes in the sediment column. This study examines the sediment composition and pore water chemistry in the three bays to better understand the microbial processes, nutrient cycling and metal release in these ecosystems.

Vertical profiles of pore water chemistry can illuminate organic decomposition processes within the sediment column. Below the oxygenated top layer of sediment, organic matter decomposes under suboxic to anoxic conditions. This process occurs as a series of reactions catalyzed by anaerobic microbial respiration that oxidize organic molecules (Kristensen 2000). The reactions involve a series of electron acceptors –  $\text{NO}_3^-$ ,  $\text{Mn}^{+4}$ ,  $\text{Fe}^{+3}$ ,  $\text{SO}_4^{-2}$  - which are sequentially reduced with depth by the following reactions:



Extent and location of each of these reactions within the sediment column can be determined based on concentrations of  $\text{NH}_4^+$ ,  $\text{Mn}^{+2}$ ,  $\text{Fe}^{+2}$ ,  $\text{SO}_4^{-2}$ , and dissolved inorganic carbon (DIC), which is approximately equivalent to  $\text{HCO}_3^-$  concentration at seawater pH.

Decomposition of organic matter may also release trace concentrations of heavy metals such as uranium into the pore water (Mangini et al. 2001, Zheng et al. 2002). Uranium may also be released by dissolution of biogenic carbonates with high uranium concentrations (Russell et al. 2004). Concentrations of uranium in the pore water are controlled both by the extent of decomposition or dissolution and by the concentration of uranium within the sediments. Decomposition also affects the pH of pore waters, which in turn controls the amount of heavy metals that can remain in solution.

Fractionation patterns of stable carbon isotopes can explain patterns of organic activity, as living organisms preferentially uptake  $^{12}\text{C}$  over  $^{13}\text{C}$ . Photosynthetic organisms preferentially remove  $^{12}\text{C}$ , enriching the seawater DIC in  $^{13}\text{C}$  and in turn increasing the  $\delta^{13}\text{C}$  in directly-precipitated carbonates. Respiring organisms, however, consume oxygen and produce carbon dioxide, enriching the seawater in  $^{12}\text{C}$  and decreasing the  $\delta^{13}\text{C}$  in seawater DIC and carbonates. (Patterson and Walter, 1994)

## METHODS

Replicate cores were collected from each sampling location for sediment and pore water analysis and for incubation experiments. Samples for microbial analysis and both organic fraction and carbonate stable carbon isotope analysis were preserved from the cores collected for sediment analysis. Pore water was extracted from the sediment by centrifugation, filtered through a 0.45µm nylon membrane, and preserved for analysis. Incubation cores were kept sealed in core tubes for at least three days after collection before being processed identically to pore water cores. Cores analyzed for trace metal concentrations were extruded and preserved in an anoxic (N<sub>2</sub>-flushed) environment to prevent oxidation of metals.

Pore water was analyzed for major anions on a Dionex 500-series Ion Chromatograph (IC), major cations on a Leeman Labs Inductively Coupled Plasma Atomic Emission Spectrophotometer (ICP-AES), and trace metals on an inductively coupled plasma mass spectrometer with an octapole collision cell (Agilent 7500ce ORS ICP-MS). Ammonia was measured using a Hach field spectrophotometer. DIC was measured using a flow injection analysis instrument designed after Hall and Aller (1992). Microbe populations in the sediment column were analyzed by extracting protein from preserved sediments using a sodium dodecyl sulfate (SDS) solution coupled with sonication. Concentrations were qualitatively determined using the BioRad RC DC Protein Assay, a colorimetric assay modified from the Lowry et al. (1951) assay. Stable carbon isotope analysis was conducted on fine fraction (<63µm) carbonate at the University of Massachusetts-Amherst and seawater DIC at the University of Michigan Stable Isotope Laboratory.

## RESULTS

Vertical profiles of protein concentrations, a rough proxy for microbial populations, indicate the highest levels of microbial activity near the sediment-water interface (Fig. 1).

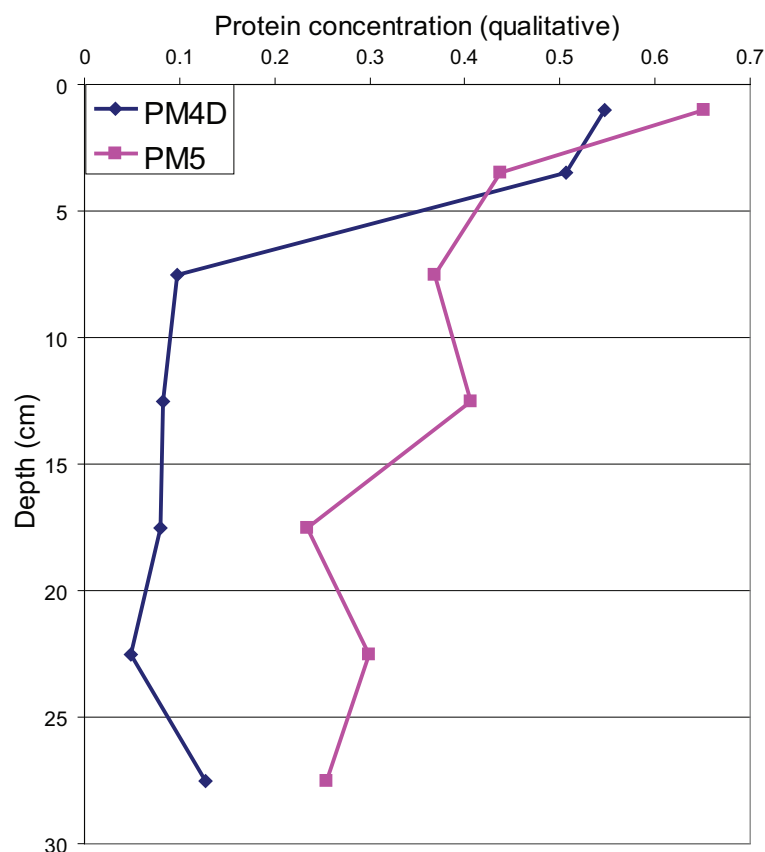
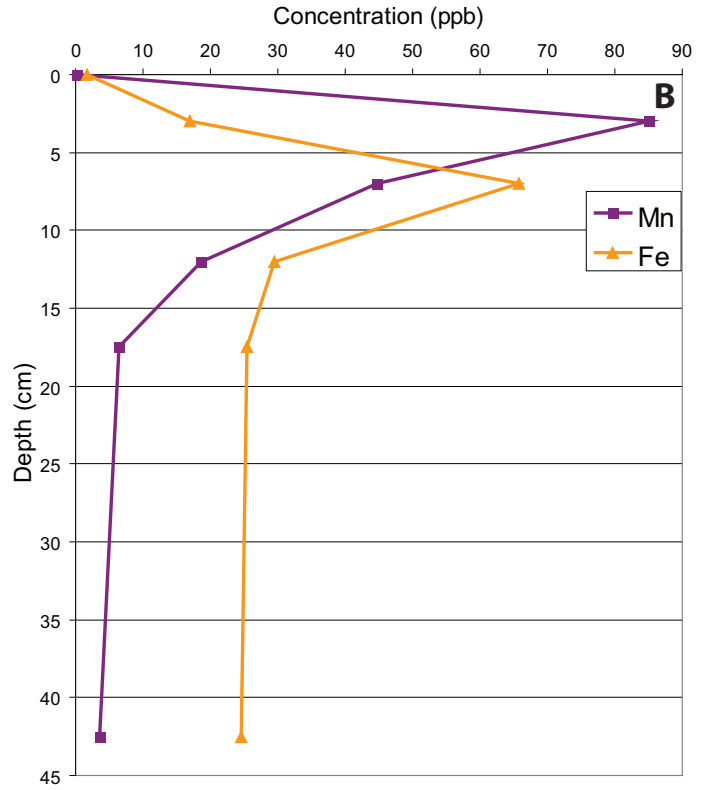
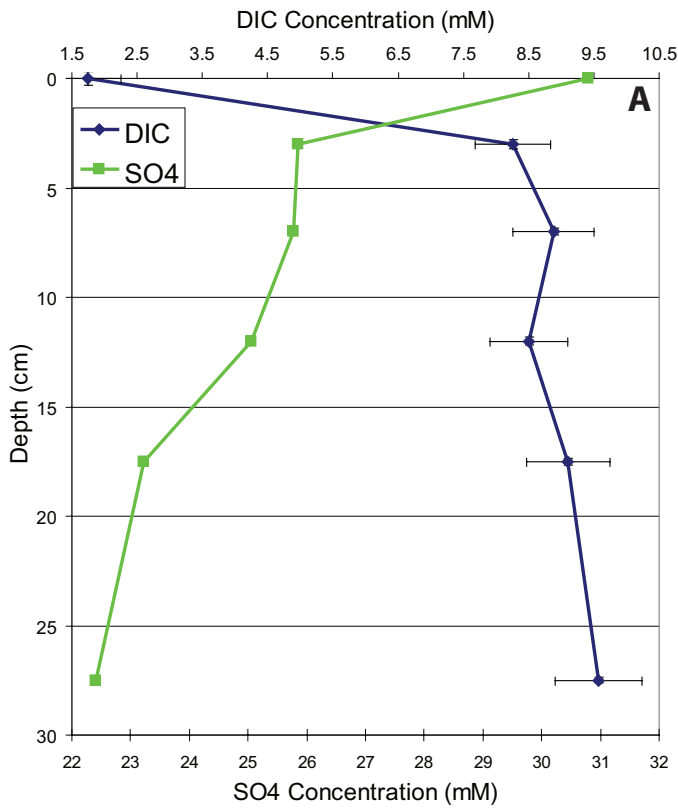


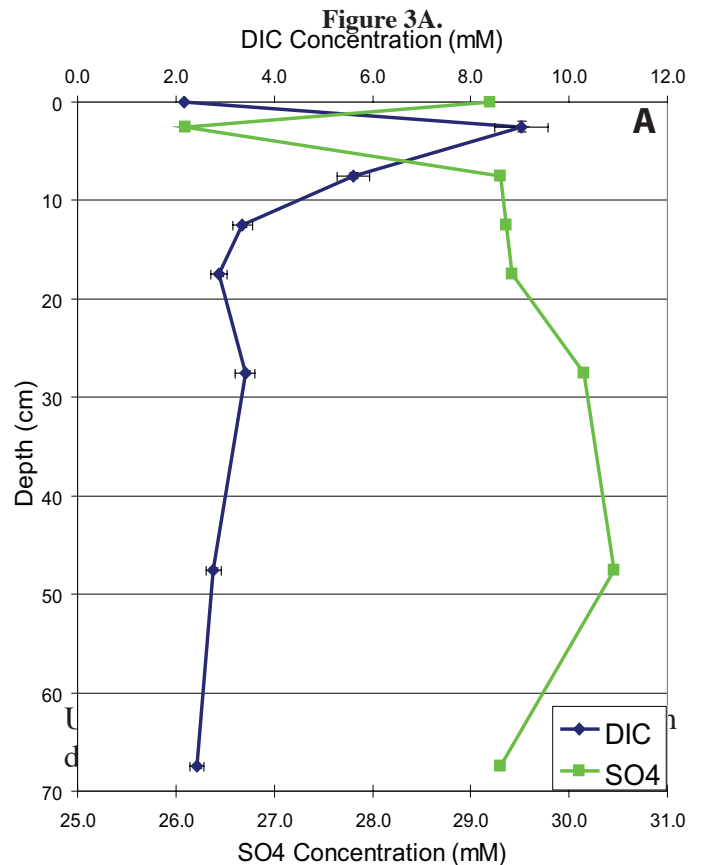
**Figure 1: Vertical profiles of protein concentrations, a rough proxy for microbial populations.**

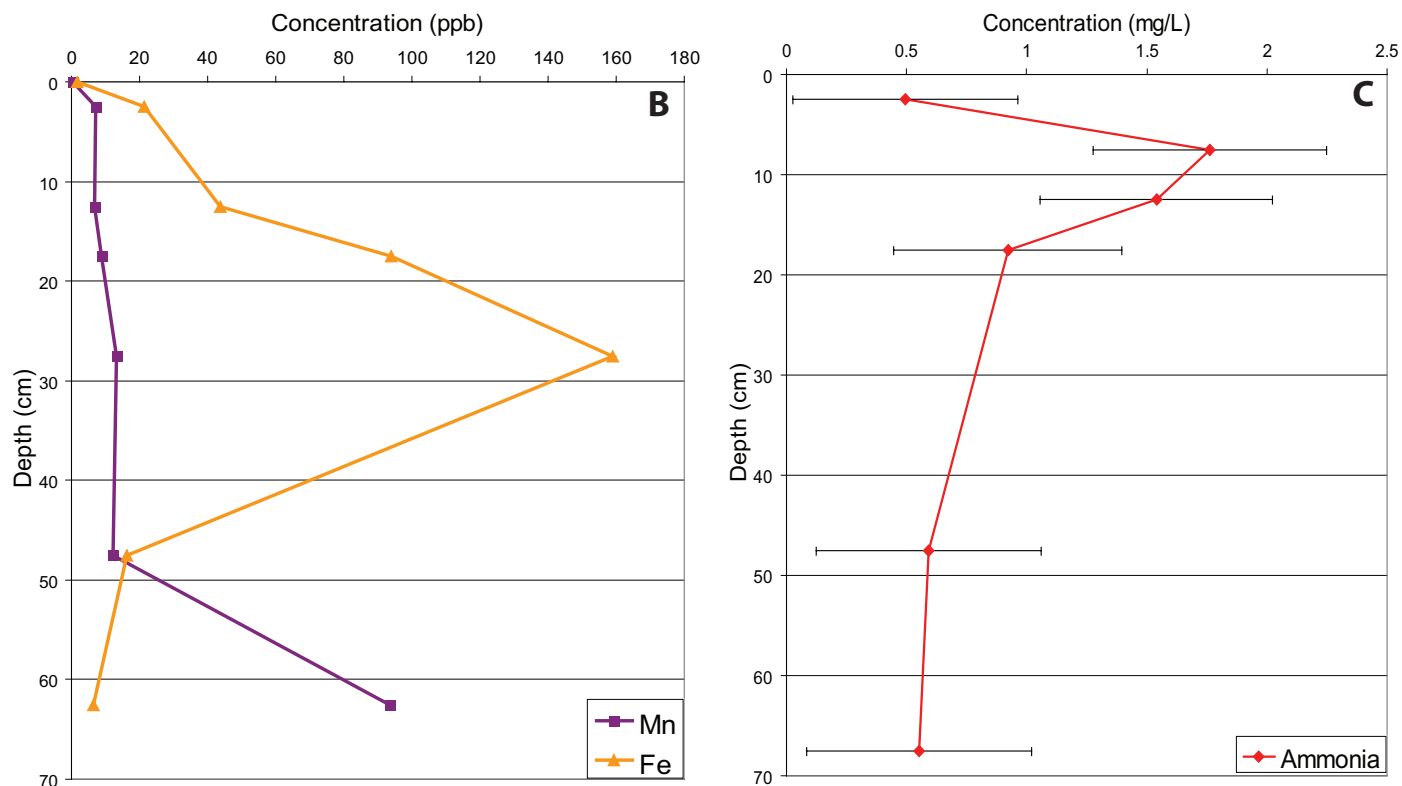
Vertical pore water profiles for deep-water environment cores (Fig. 2) show typical profiles of ion reduction expected from progressive organic matter decomposition with depth. The Mn<sup>+2</sup> concentrations peak near the sediment-water interface and Fe<sup>+2</sup> concentrations peak just below. The SO<sub>4</sub><sup>-2</sup> concentration decreases and DIC increases gradually with depth, as predicted by ongoing sulfate reduction. Nitrate reduction was not discernible based on the low resolution of the ammonia data.

**Figure 2: Vertical pore water profiles for deep-water environment core from Puerto Mosquito (PMD1) A. Sulfate concentration profile. B. Iron and manganese concentration profiles.**



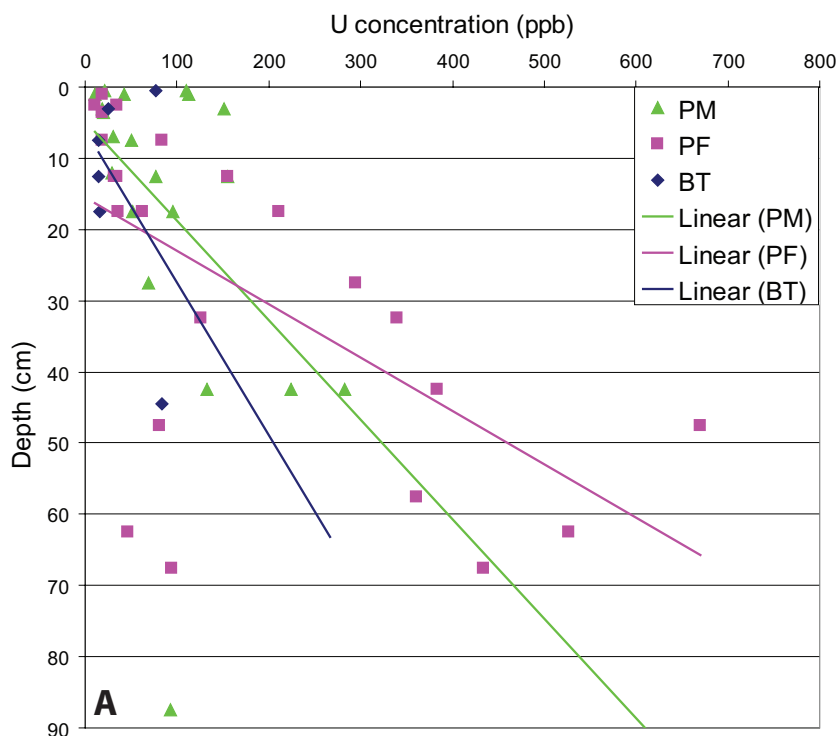
Vertical pore water profiles for shallow-water environment cores (Fig. 3) show a more complicated profile of ion reduction. Ammonia concentrations peak near the sediment-water interface.  $Mn^{+2}$  and  $Fe^{+2}$  concentrations generally increase more gradually with depth than the steep peaks evident in deep-environment cores and peaks occur deeper within the cores. Just below the sediment-water interface,  $SO_4^{-2}$  decreases and DIC increases sharply. With increasing depth, however,  $SO_4^{-2}$  and DIC return to concentrations close to that of the overlying seawater.





**Figure 3: Vertical pore water profiles for shallow-water environment core from Puerto Ferro (PF5). A. Sulfate concentration profile. B. Iron and manganese concentration profiles. C. Ammonia concentration profile.**

Uranium concentrations generally increase with depth within individual cores. Comparing between the bays, concentrations are generally higher in Puerto Ferro than in Puerto Mosquito and Puerto Ferro. (Fig. 4a) Incubation experiments show that uranium concentrations increase with incubation and the rate of uranium release increases with depth (Fig. 4b).



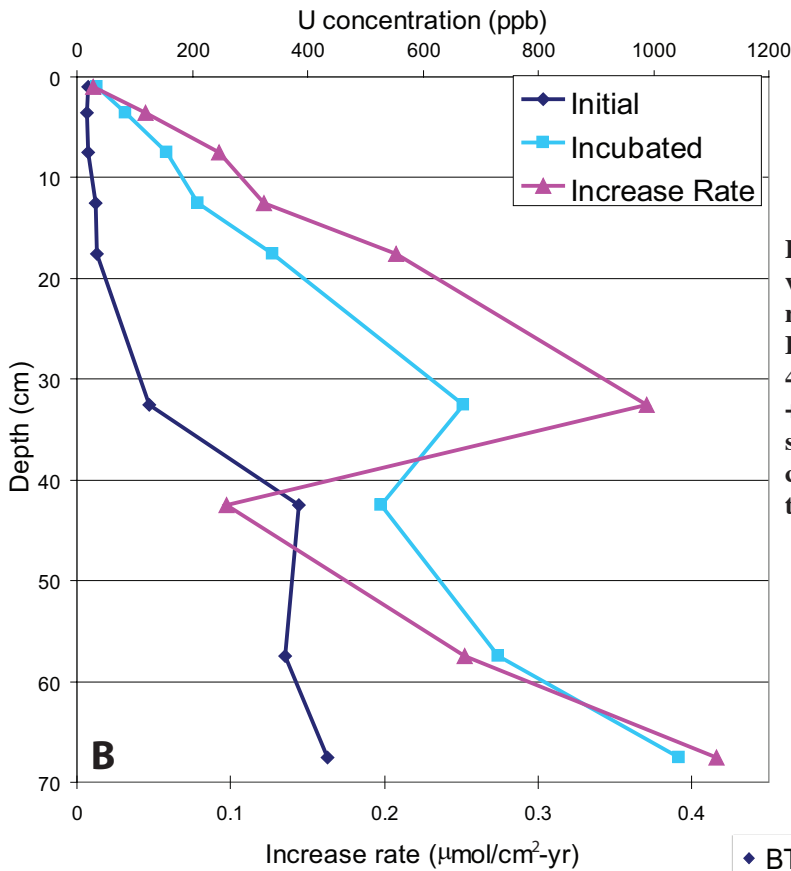


Figure 4: A. Uranium concentrations plotted versus depth in each of the three bays. Linear regression for Puerto Ferro:  $y = 0.0749x + 15.528$ ;  $R^2 = 0.3738$ ; for Puerto Mosquito:  $y = 0.1397x + 4.7391$ ,  $R^2 = 0.2126$ ; for Bahia Tapon:  $y = 0.2144x + 5.9919$ ,  $R^2 = 0.1896$ . B. Uranium profile for shallow-water core in Puerto Ferro (PF4). Initial concentrations, concentrations after 6-day incubation, and uranium release rate.

Comparison of  $\delta^{13}\text{C}$  from carbonate sediments between the three bays indicates that Puerto Mosquito sediments are depleted in  $^{13}\text{C}$  relative to Puerto Ferro and Bahia Tapon. Overlying seawater DIC tracks the same trend, with the most  $^{13}\text{C}$ -depleted carbon in Puerto Mosquito. (Fig. 5a) Organic carbon isotope ratios in the three bays also tracks the same trend, with the most negative  $\delta^{13}\text{C}$  signature on organic matter from Puerto Mosquito. (Fig. 5b)

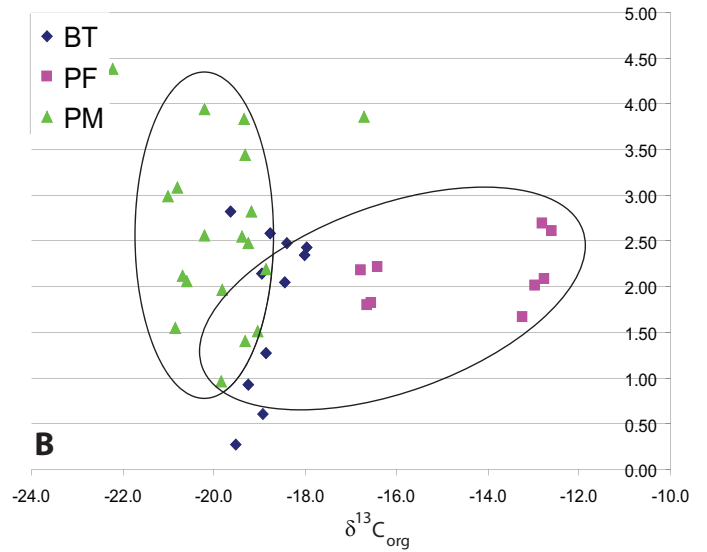
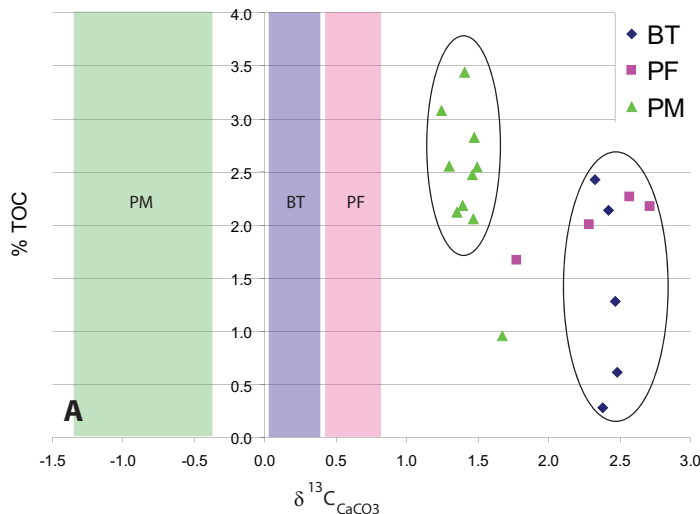


Figure 5: Stable carbon isotope distributions. A. Total organic carbon (TOC) is plotted versus  $\delta^{13}\text{C}$  from fine fraction ( $<63\mu\text{m}$ )  $\text{CaCO}_3$  from the top 30cm of all three bays, with circles highlighting the differentiation between Puerto Mosquito and the other two bays. Shaded regions indicate the average  $\pm 0.5$  standard deviation of  $\delta^{13}\text{C}$  of DIC in seawater from each bay. B. TOC is plotted versus  $\delta^{13}\text{C}$  from organic matter in all three bays with circles highlighting the differentiation between Puerto Mosquito and the other two bays.

## DISCUSSION AND CONCLUSIONS

Relative measurements of protein concentrations in shallow cores (Fig. 1) indicate the highest levels of microbial activity near the sediment-water interface, suggesting the highest rates of microbial catalysis of organic matter decomposition in the organic-rich top intervals.

Vertical pore water profiles from deep bay cores (Fig. 2) indicate progressive sulfate reduction and Mn and Fe reduction zones in the top 20cm of sediment. This is consistent with suboxic-anoxic organic matter decomposition combined with restricted pore water flow in fine-grained sediments, which prevents the ions produced in peak reduction zones from spreading throughout the core.

Vertical pore water profiles from shallow bay cores (Fig. 3) show inverse profiles of classic sulfate reduction and Fe and Mn reduction zones deeper in the sediment profile than in the deep-environment cores. The deeper Fe and Mn reduction zones (Fig. 3b) are consistent with less restricted pore water flow in permeable sediments with a shell-rich matrix and high bioturbation, spreading the transition from oxic to suboxic and anoxic conditions throughout a larger depth range. The  $\text{NH}_4^+$  peak is likely evident in shallow water but not deep water cores due to this shift of each of the reduction zones deeper in the core, translating the nitrate reduction zone to a range measurable within the resolution of this study. The sulfate reduction profile (Fig. 3a) can be explained by particularly active sulfate reduction near the sediment-water interface as a result of rapid organic matter decomposition in this interval. The apparent lack of sulfate reduction at depth is likely the result of transport processes in sediments with relatively unrestricted pore water flow, allowing sufficient sulfate ion transfer throughout the core to produce sulfate concentrations comparable to the open ocean at depth.

The vertical profile of uranium release with incubation at site PF4 (Fig. 4b) suggests a source of uranium from within the sediment column, either from organic matter decomposition or from carbonate dissolution. The release rates continue to increase with depth to 35cm, below the region of most active organic matter decomposition, and do not return to the low rates of uranium release at the surface even down to 70cm, suggesting either a uranium source from sediments that are breaking down more rapidly with depth or a more concentrated source of uranium in deeper sediments. Since uranium concentrations increase with depth in all three bays (Fig. 4a), it seems most likely that the uranium concentration within the source sediments is increasing with depth. Higher uranium concentrations in Puerto Ferro sediments than in the other two bays may also be a result of twentieth century U.S. Navy bombing tests with U-depleted shells on the island of Vieques (Murillo 2001).

The lower  $\delta^{13}\text{C}$  in both carbonate sediments and overlying seawater DIC in Puerto Mosquito than the other two bays (Fig. 5a) suggest either lower rates of primary productivity (autotrophic photosynthesizing organisms) or higher rates of heterotrophic (respiring organism) growth. The higher levels of total organic carbon in Puerto Mosquito sediments and the high concentrations of dinoflagellates, a heterotrophic organism, suggest that the  $^{13}\text{C}$  depletion is the result of increased heterotrophic growth, not lower primary productivity. The corresponding trend of increasingly negative  $\delta^{13}\text{C}$  in organic carbon from Puerto Mosquito (Fig. 5b) may similarly be a product of high levels of heterotrophic organic activity or may reflect the isotopic signature of the primary producers in the bay.

## REFERENCES

sediments by bioturbation. *Geochimica et Cosmochimica Acta*, 66, 10, 1759-1772.

Hall, P.O.J. and Aller, R.C. 1992. Rapid, small-volume, flow injection analysis for  $\Sigma\text{CO}_2$  and  $\text{NH}_4^+$  in marine and freshwaters. *Limnology and Oceanography*, 37, 5, 1113-1119.

Kristensen, E. 2000. Organic matter diagenesis at the oxic/anoxic interface in coastal marine sediments, with emphasis on the role of burrowing animals. *Hydrobiologia*, 426, 1, 1-24.

Lowry, O.H., Rosebrough, N.J., Farr, A.L., and Randall R.J. 1951. Protein measurement with the Folin phenol reagent. *J. Biol. Chem.*, 193, 265-275.

Mangini, A., Jung, M., and Laukenmann, S. 2001. What do we learn from peaks of uranium and of manganese in deep sea sediments? *Marine Geology*, 177, 1, 63-78.

Murillo, M. 2001. *Islands of Resistance: Puerto Rico, Vieques, and U.S. Policy*. Seven Stories Press: New York, NY.

Patterson, W.P. and Walter, L.M. 1994. Depletion of  $^{13}\text{C}$  in seawater  $\Sigma\text{CO}_2$  on modern carbonate platforms: Significance for the carbon isotopic record of carbonates. *Geology*, 22, 885-888.

Russell, A.D., Honisch, B., Howard, J.S., and Lea, D.W. 2004. Effects of seawater carbonate ion concentration and temperature on shell U, Mg, and Sr in cultured planktonic foraminifera. *Geochimica et Cosmochimica Acta*, 68, 21, 4347-4361.

Zheng, Y., Anderson, R.F., van Geen, A. and Fleisher M.Q. 2002. Remobilization of authigenic uranium in marine